SOIL Discuss., 2, 505–535, 2015
www.soil-discuss.net/2/505/2015/
doi:10.5194/soild-2-505-2015

SOIL Discussions
Open Access

Analysis of the linearised observation operator in a soil moisture and temperature analysis scheme

I. Dharssi[1], **B. Candy**[2], **and P. Steinle**[1]

[1]Bureau of Meteorology, Melbourne, Australia
[2]Met Office, Exeter, UK

Received: 14 April 2015 – Accepted: 15 May 2015 – Published: 1 June 2015

Correspondence to: I. Dharssi (i.dharssi@bom.gov.au)

Published by Copernicus Publications on behalf of the European Geosciences Union.

Abstract

Several weather forecasting agencies have developed advanced land data assimilation systems that, in principle, can analyse any model land variable. Such systems can make use of a wide variety of observation types, such as screen level (2 m above the surface) observations and satellite based measurements of surface soil moisture and skin temperature. Indirect measurements can be used and information propagated from the surface into the deeper soil layers. A key component of the system is the calculation of the linearised observation operator matrix (Jacobian matrix) which describes the link between the observations and the land surface model variables. The elements of the Jacobian matrix (Jacobians) are estimated using finite difference by performing short model forecasts with perturbed initial conditions. The calculated Jacobians show that there can be strong coupling between the screen level and the soil. The coupling between the screen level and surface soil moisture is found to be due to a number of processes including bare soil evaporation, soil thermal conductivity as well as transpiration by plants. Therefore, there is significant coupling both during the day and at night. The coupling between the screen level and root-zone soil moisture is primarily through transpiration by plants. Therefore the coupling is only significant during the day and the vertical variation of the coupling is modulated by the vegetation root depths. The calculated Jacobians that link screen level temperature to model soil temperature are found to be largest for the topmost model soil layer and become very small for the lower soil layers. These values are largest during the night and generally positive in value. It is found that the Jacobians that link observations of surface soil moisture to model soil moisture are strongly affected by the soil hydraulic conductivity. Generally, for the Joint UK Land Environment Simulator (JULES) land surface model, the coupling between the surface and root zone soil moisture is weak. Finally, the Jacobians linking observations of skin temperature to model soil temperature and moisture are calculated. These Jacobians are found to have a similar spatial pattern to the Jacobians for

SOILD

2, 505–535, 2015

observations of screen level temperature. Analysis is also performed of the sensitivity of the calculated Jacobians to the magnitude of the perturbations used.

1 Introduction

Many observational and modelling studies suggest strong coupling between the atmosphere and the land surface. The land surface states such as soil moisture, temperature and snow play an important role in land-atmosphere coupling. The very high albedo of snow, as well as the water storage and insulation properties means that snow can have a significant impact on numerical weather prediction (NWP) and seasonal forecasting. Soil moisture and temperature have a significant impact on screen level temperature and humidity, low clouds and precipitation, by influencing the exchange of heat and moisture between the land surface and the atmosphere (Schneider et al., 2014; Walker and Rowntree, 1977; Timbal et al., 2002). Soil moisture is important for the prediction of summer-time precipitation at mid-latitudes over land and plays an important role in the development of convective storms (Findell and Eltahir, 1997). The land surface is also very important for the seasonal prediction of extreme events such as heat waves and drought (Weisheimer et al., 2011).

Data assimilation (DA) is extremely important for NWP since errors in the model initial conditions can grow rapidly and seriously degrade forecasts. The initial land surface state can have a significant impact on forecasts of screen level temperature and humidity as well as forecasts of precipitation. Specifying the model initial soil moisture and temperature state is especially difficult since there are few near real-time ground based observations of soil moisture and temperature. Therefore, indirect observations are usually used by land surface DA schemes to initialise the model soil moisture and temperature (Dharssi et al., 2011; de Rosnay et al., 2012). The true information content of soil moisture data is in the relative values (such as temporal variations or percent of saturation) and not in the absolute magnitudes (Brocca et al., 2014). Consequently, model soil moisture is highly model specific. For example, Koster et al. (2009) show

SOILD
2, 505–535, 2015

that direct transfer of soil moisture values from one land surface model to a different land surface model is inappropriate and likely to lead to problems. Therefore, any land surface DA scheme must be consistent with the land surface model used by the NWP system. Inconsistencies in the analysed land surface fields could introduce spurious, long lived shocks to the NWP system and degrade forecasts.

To make fuller use of the available global remotely sensed measurements of the land surface as well as screen level observations an Extended Kalman Filter (EKF) based land surface data assimilation system has been developed in collaboration between the Bureau of Meteorology (Bureau) and the Met Office (Dharssi et al., 2012). Such EKF land DA systems can make more statistically optimal use of a wide variety of observation types, such as screen level observations and satellite based estimates such as retrieved Surface Soil Moisture, retrieved skin temperature, Leaf Area Index (LAI) and Fraction of Photosynthetically Active Radiation. Indirect measurements can be used and information propagated from the surface into the deeper soil layers. For example an EKF based land DA system may: (a) use observations of screen level temperature and humidity to analyse soil temperature and moisture. (b) Use satellite estimates of surface soil moisture to analyse surface and root-zone soil moisture. (c) Use satellite estimates of skin temperature to analyse soil temperature and moisture. (d) Assimilate satellite estimates of LAI (Rudiger et al., 2010).

2 Land surface analysis

A number of new space-borne remote sensing systems have been developed that provide information on surface soil moisture and temperature. However, most NWP centres still only use screen level observations of temperature and humidity for the operational analysis of soil moisture and temperature, e.g. ECMWF (European Centre for Medium range Weather Forecasts; de Rosnay et al., 2012), Meteo-France (Giard and Bazile, 2000) and the German Weather Service (Hess et al., 2008). The Met Office operationally uses satellite derived measurements of surface soil wetness together with

SOILD
2, 505–535, 2015

screen level observations for the analysis of soil moisture. Dharssi et al. (2011) find that assimilation of remotely sensed surface soil wetness measurements improves the agreement of the soil moisture analyses with ground based soil moisture observations and improves forecasts of screen level temperature and humidity.

2.1 The extended Kalman filter

The DA problem is kept manageable by assuming that the model land columns are independent of each other (a 1-dimensional approach). This assumption is also made by most land surface models, including JULES (Best et al., 2011). The standard EKF equations for each land column are given by

$$\mathbf{x^a}(t_i) = \mathbf{x^b}(t_i) + \mathbf{K}_i \left[\mathbf{o}(t_i) - h_i(\mathbf{x^b})\right] \quad (1)$$

$$\mathbf{K}_i = \mathbf{B}\mathbf{H}_i^T \left(\mathbf{H}_i \mathbf{B}\mathbf{H}_i^T + \mathbf{R}\right)^{-1} . \quad (2)$$

$\mathbf{x}(t_i)$ represents the state vector of a land column at time t_i with superscripts a and b standing for analysis and background. $\mathbf{o}(t_i)$ is the observation vector. $\mathbf{K}_i$ is the Kalman gain matrix at time t_i. $\mathbf{B}$ is the background error covariance matrix. $\mathbf{R}$ is the observation error covariance matrix.

$\mathbf{H}_i$ is the linearised observation operator matrix and is defined using $h_i(\mathbf{x}+\mathbf{\Delta}) \simeq h_i(\mathbf{x}) + \mathbf{H}_i\mathbf{\Delta}$, where $\mathbf{\Delta}$ is a small perturbation to the model state $\mathbf{x}$ and $h_i(\mathbf{x})$ is the non-linear observation operator. The elements of $\mathbf{H}_i$ are estimated using finite difference by individually perturbing each component of $\mathbf{x}$ by a a small scalar amount δ_j. A given element of $\mathbf{H}_i$ is calculated using

$$H_{kj} = \frac{y_k(\mathbf{x}+\delta_j) - y_k(\mathbf{x})}{\delta_j}. \quad (3)$$

SOILD
2, 505–535, 2015

$y_k(\mathbf{x}+\delta_j)$ is a short model forecast of observation type k (e.g. screen level temperature) starting from perturbed initial conditions $\mathbf{x}+\delta_j$. The sensitivity of the calculated Jacobians to the magnitude of the perturbations, δ, is described in a later subsection. The number of perturbed forecasts required increases with the number of model variables to be analyses and the number of soil layers. For example, to analyse skin temperature and soil moisture and temperature on four soil levels would require ten perturbed forecasts, including the control $y(\mathbf{x})$. The length of a perturbed forecast is typically a few hours long.

The major computational cost of the EKF land DA system is the cost of running the perturbed forecasts. ECMWF (de Rosnay et al., 2012) use the fully coupled land/atmosphere model for the perturbed forecasts. Meteo France (Mahfouf et al., 2009) use an off-line land surface model (uncoupled to the atmosphere model) for the perturbed forecasts. Consequently the Meteo France EKF land DA system is computationally several orders of magnitude cheaper. The Bureau EKF land DA system also uses an off-line land surface model for the perturbation forecasts. Balsamo et al. (2007) and Mahfouf et al. (2009) have shown that the off line land surface model can be used to reliably calculate $\mathbf{H}_j$. The forcing data for the off-line land surface model (precipitation, surface longwave and shortwave radiation, air temperature and humidity, wind speed and surface pressure) are obtained from forecasts of the NWP model. Air temperature and humidity forcing are applied at a height of 20 m (which is above the screen level). This allows the EKF land DA system to also assimilate observations of screen level temperature and humidity (see Fig. 1 of Mahfouf et al., 2009, for a fuller explanation).

2.2 The land surface model

The Bureau EKF land DA system uses JULES to represent the land surface processes. The soil is discretised into four layers of 0.1, 0.25, 0.65 and 2 m thickness (from top to bottom). The soil hydrology is based on a finite difference form of the Richards equation and Darcy's law. The van Genuchten (1980) equations are used to describe

SOILD
2, 505–535, 2015

the relationship of soil hydraulic conductivity and soil suction to the unfrozen volumetric soil moisture. Currently, there is no vertical variation of the soil hydraulic parameters in the model. The freezing and melting of soil water are also represented and the associated latent heat is included in the thermodynamic calculations.

The JULES model uses 5 vegetation tiles (broadleaf trees, needleleaf trees, C3 (temperate) grass, C4 (tropical) grass and shrubs) and 4 non-vegetation tiles (urban, inland open water, bare soil and land ice). Transpiration by plants extracts soil water directly from the soil layers via the plant roots while bare soil evaporation extracts soil water from the top soil layer only. The ability of plants to access water from each soil layer is determined by the root density distribution and soil moisture availability. The broadleaf trees are assumed to have a root depth of $d_r = 3\,\mathrm{m}$, needleleaf trees have $d_r = 1\,\mathrm{m}$, grasses and shrubs have $d_r = 0.5\,\mathrm{m}$ and the total depth of the model soil $z_t = 3\,\mathrm{m}$. The bulk stomatal resistance in the absence of soil moisture stress is calculated by a photosynthesis model (Mercado et al., 2007) and depends on incident radiation, vegetation type, surface air temperature and humidity deficit. The bulk stomatal resistance includes a dependency on the soil moisture content via a soil moisture availability factor.

3 Experiments and results

In order to avoid compensating effects through temporal averaging, results are presented for one time period only; the off-line perturbed forecasts are started from initial conditions valid at 3Z 16 January 2011. The length of the perturbed forecasts is three hours. Perturbed forecasts with shorter (longer) lengths of one (five) hour(s) have also been tried. Figure 1 shows the model initial conditions for snow amount and level 1 soil temperature. During January much of the Northern Hemisphere land is covered by snow. The initial land surface model states (e.g. soil moisture, soil temperature and snow) used in the experiments are obtained from the operational weather forecasting system and are as accurate as possible. Although the model initial conditions are likely to affect the magnitude of the computed Jacobians, they do not affect the conclusions.

SOILD
2, 505–535, 2015

3.1 The Jacobians for screen level observations

Figure 2 shows an example of the computed Jacobians $H_{T_{2\,\mathrm{m}},\theta_l} \equiv \Delta T_{2\,\mathrm{m}}/\Delta\theta_l$ which are elements of the linearised observation operator matrix for screen level temperature with respect to soil moisture in the four model soil layers (l). For soil layers two to four, the coupling between screen level temperature and soil moisture is primarily through transpiration by vegetation. Consequently the coupling occurs during daylight. The vertical variation of the coupling is discussed in the next subsection. The negative values means that an increase in soil moisture leads to a cooling of the screen level. For the surface soil layer, the picture is more complicated as there is strong coupling both during the day and at night. The Jacobians have a positive value in some places and a negative value in others.

The Jacobians of screen level specific humidity with respect to soil moisture ($\Delta q_{2\,\mathrm{m}}/\Delta\theta_l$) are shown in Fig. 3. The spatial pattern shown in Fig. 3 is similar to Fig. 2. However, for screen level specific humidity, the Jacobian values are primarily positive meaning that an increase in soil moisture leads to an increase in screen level humidity.

The Jacobians of screen level temperature with respect to soil temperature ($\Delta T_{2\,\mathrm{m}}/\Delta T_l$) are shown in Fig. 4. The Jacobians are largest for soil level 1 and become very small for soil levels 3 and 4. The Jacobians are largest during the night and generally positive in value. This is consistent with the experience of ECMWF who find that their soil temperature nudging scheme is more effective during the night and winter when screen level errors are less likely to be related to soil moisture (Mahfouf et al., 2000).

Effect of land surface parameterisations

To investigate the impact of the land surface model parameterisations on the calculation of the Jacobians, experiments are performed where the parameterisations are modified or switched off. Figure 5 shows the effect of switching off bare soil evaporation. Comparing Fig. 5 with the top panel of Fig. 2 shows that bare soil evaporation can pro-

SOILD
2, 505–535, 2015

duce strong coupling between screen level temperature and surface soil moisture, both during the day and night. Switching off bare soil evaporation reduces the magnitude of $\Delta T_{2\,\mathrm{m}}/\Delta\theta_1$ in the interior of Australia, the Sahara and parts of south America. In some night time regions, switching off bare soil evaporation causes $\Delta T_{2\,\mathrm{m}}/\Delta\theta_1$ to swap sign and have positive instead of negative values. With bare soil evaporation switched off, $\Delta T_{2\,\mathrm{m}}/\Delta\theta_1$ is predominantly negative in the daytime region and predominantly positive in the night time region.

The soil thermal conductivity can be strongly affected by soil moisture and could be responsible for the positive values of $\Delta T_{2\,\mathrm{m}}/\Delta\theta_1$ in night-time regions, observed in Fig. 5. The JULES soil thermal conductivity (λ_s) is calculated using (Peters-Lidard et al., 1998; Dharssi et al., 2009)

$$\lambda_\mathrm{s} = (\lambda_\mathrm{sat} - \lambda_\mathrm{dry})Ke + \lambda_\mathrm{dry} \tag{4}$$

where λ_sat is the soil thermal conductivity when the soil is saturated and λ_dry when the soil is dry. Ke is the Kersten number given by

$$Ke = \begin{cases} \log_{10}\dfrac{\theta}{\theta_\mathrm{s}} + 1.0 & \dfrac{\theta}{\theta_\mathrm{s}} \geq 0.1 \\ 0 & \text{otherwise} \end{cases} . \tag{5}$$

For investigation, the parameterisation of soil thermal conductivity is modified to becomes independent of soil moisture,

$$\lambda_\mathrm{s}^\mathrm{modified} = (\lambda_\mathrm{sat} + \lambda_\mathrm{dry})/2 \ . \tag{6}$$

Figure 6 shows $\Delta T_{2\,\mathrm{m}}/\Delta\theta_1$ when the soil thermal conductivity parameterisation is modified and bare soil evaporation is switched off. Comparing Figs. 5 and 6 shows that modifying soil thermal conductivity significantly reduces the coupling between screen level temperature and topmost level soil moisture in many regions, both during the day and

SOILD
2, 505–535, 2015

night. However, some night-time regions with positive values of $\Delta T_{2\,\mathrm{m}}/\Delta\theta_1$ still persist. This suggests that other processes, such as the relation between soil heat capacity and soil moisture, are also important.

The coupling between the root zone soil moisture and the screen level is primarily through transpiration by plants and is only significant during the day. The vertical variation of the coupling is significantly affected by the vegetation root depths. Figure 7 shows the computed Jacobians $\Delta T_{2\,\mathrm{m}}/\Delta\theta_l$ when the vegetation root depths are doubled. Increasing the vegetation root depth causes stronger coupling with the deeper soil layers, i.e. increases the magnitude of $\Delta T_{2\,\mathrm{m}}/\Delta\theta_4$ and reduces the magnitude of $\Delta T_{2\,\mathrm{m}}/\Delta\theta_2$.

3.2 The Jacobians for the assimilation of surface soil moisture measurements

Several new space-borne remote sensing systems have been developed that provide global retrievals of surface soil moisture (SSM), e.g. SMOS (Soil Moisture Ocean Salinity, Kerr et al., 2001), ASCAT (Advanced SCATterometer, Naeimi et al., 2009) and SMAP (Soil Moisture Active Passive, Entekhabi et al., 2010). Measurements of SSM can be assimilated to update both the model surface and root zone soil moisture by using Eq. (3) to compute $\Delta\theta_1/\Delta\theta_l \equiv H_{\theta_1,\theta_l}$. Example results are shown in Fig. 8. Generally, for JULES, the coupling between the surface and root zone soil moisture is weak. $\Delta\theta_1/\Delta\theta_3$ and $\Delta\theta_1/\Delta\theta_4$ are close to zero. $\Delta\theta_1/\Delta\theta_2$ is non-zero in regions where the soil is wet and consequently the hydraulic conductivity is high. $\Delta\theta_1/\Delta\theta_1 \equiv H_{\theta_1,\theta_1}$ is close to unity in most regions, the exceptions are where the soil is wet and Jacobian values as low as 0.5 can occur. Increasing the length of the perturbation forecasts is found to significantly increase the coupling between the surface and root zone soil moisture. Draper (2011) has found similar results when using JULES.

The van Genuchten (1980) equations describe the relationship between the soil hydraulic conductivity (K_{VG}) and the unfrozen volumetric soil moisture θ^{u}.

$$K_{\mathrm{VG}} = K_{\mathrm{s}} S_{\mathrm{e}}^{L} \left[1 - (1 - S_{\mathrm{e}}^{1/m})^{m}\right]^{2}, \tag{7}$$

SOILD
2, 505–535, 2015

where the soil wetness $S_e = (\theta^u - \theta_r)/(\theta_s - \theta_r)$, $L = 0.5$ and $m = 1 - 1/n$. θ_s, θ_r, K_s, α and n are the van Genuchten soil parameters and assumed to depend on soil type. The hydraulic conductivity is very sensitive to changes in soil moisture. Small changes in soil moisture can lead to order of magnitude changes in soil hydraulic conductivity. For example, when $S_e = 1$, $K_{VG} = K_s$ while when $S_e = 0.9$ and $n = 1.18$, $K_{VG} = K_s \times 10^{-2}$. In addition, K_s is strongly affected by soil type and has a high spatial variability (see for example Marthews et al., 2014; Bandara et al., 2015). For coarse textured soils the model assumes $K_s = 1.95 \times 10^{-2}\,\mathrm{mm\,s^{-1}}$ while for medium textured soils $K_s = 2.8 \times 10^{-3}\,\mathrm{mm\,s^{-1}}$. Cosby et al. (1984); Schaap and Leij (1998) also show that the uncertainty in predicted K_s is about one order of magnitude. Consequently, uncertainty in soil type and pedotransfer functions can also lead to order of magnitude uncertainty in soil hydraulic conductivity.

Figure 9 shows the computed Jacobians $\Delta\theta_1/\Delta\theta_2$ when the soil hydraulic conductivity is increased by a factor of ten. The coupling between the SSM and the root zone has increased significantly.

Using four different land surface models with different coupling strengths and synthetic observations of SSM, Kumar et al. (2009) find that the potential of SSM assimilation to improve root zone soil moisture is higher when the coupling between the SSM and root zone soil moisture is stronger. Given that the true strength of coupling between the SSM and root zone soil moisture is unknown, the non-identical twin, assimilation experiments of Kumar et al. (2009) suggest that it is better to over-estimate rather than under-estimate the coupling between the SSM and root zone soil moisture. Therefore, artificially increasing the model soil hydraulic conductivity by a factor of ten may be an effective technique to improve the assimilation of satellite derived SSM. However, careful and comprehensive testing will be required to fully validate all the consequences of such an approach.

SOILD
2, 505–535, 2015

3.3 The Jacobians of the observation operator for surface skin temperature

Best and Maisey (2002) show that in unstable conditions, to a good approximation

$$\Delta T_* = \Delta T_{2\,\mathrm{m}} / \left(1 - \mu\, r_{\mathrm{a},2\,\mathrm{m}} / r_{\mathrm{a}}\right) \quad . \tag{8}$$

Where r_{a} ($r_{\mathrm{a},2\,\mathrm{m}}$) is the aerodynamic resistance between the surface and first model level (screen level) and $\mu \simeq 0.9$. Therefore, it is expected that the computed Jacobians between surface skin temperature and soil moisture ($\Delta T_*/\Delta\theta_l$) should show a similar spatial pattern to the Jacobians between screen level temperature and soil moisture ($\Delta T_{2\,\mathrm{m}}/\Delta\theta_l$) but have a larger magnitude (since the denominator in Eq. (8) is less than 1). Figure 10 shows the computed Jacobians $\Delta T_*/\Delta\theta_l$ and that there is significant coupling between surface skin temperature and soil moisture. Therefore, it may be possible to assimilate satellite measurements of T_* to analyse soil moisture. However, for a variety of reasons, model and satellite derived surface skin temperature exhibit very different climatologies and consequently bias correction will be required (Reichle et al., 2010). As expected, comparing Figs. 10 and 2 shows that, the spatial variation of $\Delta T_*/\Delta\theta_l$ is very similar to $\Delta T_{2\,\mathrm{m}}/\Delta\theta_l$ and the magnitudes are much larger. Figure 11 shows the computed Jacobians $\Delta T_*/\Delta T_l$ and that there is significant coupling between surface skin temperature and model level 1 soil temperature. There are also strong similarities between $\Delta T_*/\Delta T_l$ and $\Delta T_{2\,\mathrm{m}}/\Delta T_l$. Ghent et al. (2010) have assimilated measurements of surface skin temperature for the Africa region using the JULES land surface model and found improvements to model surface fluxes and soil moisture.

3.4 Sensitivity to magnitude of perturbations

Figure 12 shows the sensitivity of the calculated Jacobians for screen level temperature to the magnitude of the volumetric soil moisture perturbations, for the Australia region. The results indicates that the system is well behaved for perturbation values in the range of 10^{-4} to $10^{-2}\,\mathrm{m}^3\,\mathrm{m}^{-3}$, a perturbation value of $10^{-3}\,\mathrm{m}^3\,\mathrm{m}^{-3}$ is found to be close to optimal. A similar analysis using the calculated Jacobians for screen level specific

SOILD
2, 505–535, 2015

humidity also shows that a soil moisture perturbation value of $10^{-3}\,m^3\,m^{-3}$ is close to optimal (results not shown). The Jacobians for screen level specific humidity are less sensitive to the magnitude of the soil moisture perturbation. For skin and soil temperature, results indicate that the system is well behaved for perturbation values in the range of 10^{-2} to 1 K, a perturbation value of 10^{-1} K is found to be close to optimal.

4 Conclusions

To take full advantage of the available global satellite measurements of the land surface as well as screen level observations an EKF based land surface data assimilation system has been developed at the Bureau in collaboration with the Met Office. Such a system is flexible and can make more statistically optimal use of a wide variety of observation types. The most important aspect of the system is the calculation of the Jacobians that describe the link between the observations and the land surface model variables. The Jacobians are computed using finite difference by perturbing each model variable to be analysed, in-turn, and performing short model forecasts. The number of perturbed forecasts required increases with the number of model variables to be analyses and the number of soil layers. Other works such as Mahfouf et al. (2009) and Drusch et al. (2009) have also looked at the calculation of the Jacobians. However, this work examines the Jacobians in much greater detail than before. In addition, this is the first work to use the JULES land surface model to compute the Jacobians for screen level observations and measurements of surface skin temperature.

Results show that the computed Jacobians can be sensitive to the size of the perturbations used. Perturbations that are too small cause problems due to numerical rounding while perturbations that are too large cause problems due to non-linearities in the model. Experiments show that volumetric soil moisture perturbation values in the range of 10^{-4} to $10^{-2}\,m^3\,m^{-3}$ give good results and a perturbation value of $10^{-3}\,m^3\,m^{-3}$ is close to optimal. For skin and soil temperature perturbations, experiments indicate that a perturbation value of 10^{-1} K is close to optimal.

SOILD
2, 505–535, 2015

This is the first work to look at the effect of land surface parameterisations on the computed Jacobians. As expected, the parameterisation details have a significant impact. Experiments are performed where the parameterisations are modified or switched off. Results show that the coupling between the soil moisture in the topmost model layer and the screen level is due to a number of processes including bare soil evaporation, soil thermal conductivity, soil thermal capacity as well as transpiration by plants. The coupling between the soil moisture in the lower model layers and the screen level is due to transpiration by plants. This result is significant as it explains why the coupling with the soil moisture in the topmost model layer is much stronger than the coupling with the soil moisture in the lower model layers. Consequently, soil moisture increments in the topmost model layer will be larger than would be the case if the coupling were only due to transpiration. In addition, improving the analysis of topmost model layer soil moisture will have a significant impact on forecasts of screen level temperature and humidity.

The Jacobians linking observations of surface soil moisture with soil moisture in the lower model layers have been computed. Experiments show that artificially increasing the soil hydraulic conductivity by a factor of ten significantly increases the coupling between the surface and root zone soil moisture. Otherwise, for JULES, the coupling between the surface and root zone soil moisture is weak. Small uncertainty in soil moisture or soil type can lead to order of magnitude uncertainty in soil hydraulic conductivity. In addition, Kumar et al. (2009) suggest that it is better to over-estimate rather than under-estimate the coupling between the surface and root zone soil moisture. Consequently, artificially increasing the model soil hydraulic conductivity by a factor of ten may be an effective technique to improve the assimilation of satellite derived surface soil moisture.

The Jacobians linking observations of skin temperature to model soil temperature and moisture have also been computed. These Jacobians have a similar spatial pattern to the Jacobians linking observations of screen level temperature to model soil temperature and moisture but are larger in magnitude. Consequently, assimilation of

SOILD
2, 505–535, 2015

satellite derived skin temperature may also significantly improve the analysis of model soil temperature and moisture.

It is well known that model soil moisture is model specific (Koster et al., 2009). Results indicate that the Jacobians are also model specific. Consequently, careful examination of the Jacobians might allow significant insight into the behaviour of land surface models. It is intended that the CABLE land surface model (Kowalczyk et al., 2013) will be integrated into the JULES framework (Law et al., 2012). Therefore, it would be instructive to examine and compare the Jacobians computed using CABLE, JULES and other land surface models.

Acknowledgements. Parts of this work have been previously published as a technical report (Dharssi et al., 2012).

References

Balsamo, G., Mahfouf, J., Belair, S., and Deblonde, G.: A land data assimilation system for soil moisture and temperature: an information content study, J. Hydrometeorol., 8, 1225–1242, 2007. 510

Bandara, R., Walker, J. P., Rüdiger, C., and Merlin, O.: Towards soil property retrieval from space: An application with disaggregated satellite observations, J. Hydrol., 522, 582–593, 2015. 515

Best, M. and Maisey, P.: A physically based soil moisture nudging scheme, Hadley Centre Technical Note 35, Met. Office, Exeter, UK, 2002. 516

Best, M. J., Pryor, M., Clark, D. B., Rooney, G. G., Essery, R .L. H., Ménard, C. B., Edwards, J. M., Hendry, M. A., Porson, A., Gedney, N., Mercado, L. M., Sitch, S., Blyth, E., Boucher, O., Cox, P. M., Grimmond, C. S. B., and Harding, R. J.: The Joint UK Land Environment Simulator (JULES), model description – Part 1: Energy and water fluxes, Geosci. Model Dev., 4, 677–699, doi:10.5194/gmd-4-677-2011, 2011. 509

Brocca, L., Zucco, G., Mittelbach, H., Moramarco, T., and Seneviratne, S. I.: Absolute versus temporal anomaly and percent of saturation soil moisture spatial variability for six networks worldwide, Water Resour. Res., 50, 5560–5576, doi:10.1002/2014WR015684, 2014. 507

SOILD

2, 505–535, 2015

Cosby, B., Hornberger, G., Clapp, R., and Ginn, T.: A statistical exploration of the relationships of soil moisture characteristics to the physical properties of soils, Water Resour. Res., 20, 682–690, 1984. 515

de Rosnay, P., Drusch, M., Vasiljevic, D., Balsamo, G., Albergel, C., and Isaksen, L.: A simplified Extended Kalman Filter for the global operational soil moisture analysis at ECMWF, Q. J. Roy. Meteorol. Soc., 139, 1199–1213, doi:10.1002/qj.2023, 2012. 507, 508, 510

Dharssi, I., Vidale, P., Verhoef, A., Macpherson, B., Jones, C., and Best, M.: New soil physical properties implemented in the Unified Model at PS18, Meteorology Research and Development Technical Report 528, Met. Office, Exeter, UK, http://tinyurl.com/UKMOreport528-pdf, 2009. 513

Dharssi, I., Bovis, K. J., Macpherson, B., and Jones, C. P.: Operational assimilation of ASCAT surface soil wetness at the Met Office, Hydrol. Earth Syst. Sci., 15, 2729–2746, doi:10.5194/hess-15-2729-2011, 2011. 507, 509

Dharssi, I., Steinle, P., and Candy, B.: Towards a Kalman Filter based land surface data assimilation scheme for ACCESS, CAWCR Technical Report 54, The Centre for Australian Weather and Climate Research, Melbourne, Australia, http://www.cawcr.gov.au/publications/technicalreports/CTR_054.pdf (last access: 29 May 2015), 2012. 508

Draper, C.: Near-surface Soil Moisture Assimilation in NWP, PhD thesis, Department of Civil and Environmental Engineering, University of Melbourne, Parkville, Australia, http://users.monash.edu.au/~jpwalker/theses/ClaraDraper.pdf (last access: 29 May 2015), 2011. 514

Drusch, M., Scipal, K., De Rosnay, P., Balsamo, G., Andersson, E., Bougeault, P., and Viterbo, P.: Towards a Kalman Filter based soil moisture analysis system for the operational ECMWF Integrated Forecast System, Geophys. Res. Lett, 36, L10401, doi:10.1029/2009GL037716, 2009. 517

Entekhabi, D., Njoku, E. G., O'Neill, P. E., Kellogg, K. H., Crow, W. T., Edelstein, W. N., Entin, J. K., Goodman, S. D., Jackson, T. J., Johnson, J., Kimball, J., Piepmeier, J. R., Koster, R. D., Martin, N., McDonald, K. C., Moghaddam, M., Moran, S., Reichle, R., Shi, J.-C., Spencer, M. W., Thurman, S. W., Leung, T., and Van Zyl, J.: The soil moisture active passive (SMAP) mission, Proc. IEEE, 98, 704–716, 2010. 514

Findell, K. and Eltahir, E.: An analysis of the soil moisture-rainfall feedback, based on direct observations from Illinois, Water Resour. Res., 33, 725–735, 1997. 507

SOILD
2, 505–535, 2015

Ghent, D., Kaduk, J., Remedios, J., Ardö, J., and Balzter, H.: Assimilation of land surface temperature into the land surface model JULES with an ensemble Kalman filter, J. Geophys. Res, 115, D19112, doi:10.1029/2010JD014392, 2010. 516

Giard, D. and Bazile, E.: Implementation of a new assimilation scheme for soil and surface variables in a global NWP model, Mon. Weather Rev., 128, 997–1015, 2000. 508

Hess, R., Lange, M., and Wergen, W.: Evaluation of the variational soil moisture assimilation scheme at Deutscher Wetterdienst, Q. J. Roy. Meteorol. Soc., 134, 1499–1512, doi:10.1002/qj.306, 2008. 508

Kerr, Y., Waldteufel, P., Wigneron, J., Martinuzzi, J., Font, J., and Berger, M.: Soil moisture retrieval from space: The Soil Moisture and Ocean Salinity (SMOS) mission, IEEE Trans. Geosci. Remote Sens., 39, 1729–1735, doi:10.1109/36.942551, 2001. 514

Koster, R., Guo, Z., Yang, R., Dirmeyer, P., Mitchell, K., and Puma, M.: On the nature of soil moisture in land surface models, J. Climate, 22, 4322–4335, 2009. 507, 519

Kowalczyk, E., Stevens, L., Law, R., Dix, M., Wang, Y., Harman, I., Haynes, K., Srbinovsky, J., Pak, B., and Ziehn, T.: The land surface model component of ACCESS: description and impact on the simulated surface climatology, Aust. Meteorol. Oceanogr. J., 63, 65–82, 2013. 519

Kumar, S. V., Reichle, R. H., Koster, R. D., Crow, W. T., and Peters-Lidard, C. D.: Role of Subsurface Physics in the Assimilation of Surface Soil Moisture Observations, J. Hydrometeorol., 10, 1534–1547, doi:10.1175/2009JHM1134.1, 2009. 515, 518

Law, R., Raupach, M., Abramowitz, G., Dharssi, I., Haverd, V., Pitman, A., Renzullo, L., Van Dijk, A., and Wang, Y. P.: CABLE RoadMap 2012-2017, CAWCR Technical Report, The Centre for Australian Weather and Climate Research, Australia, 2012. 519

Mahfouf, J., Viterbo, P., Douville, H., Beljaars, A., and Saarinen, S.: A revised land-surface analysis scheme in the integrated forecasting system, ECMWF newsletter, 88, 8–13, http://old.ecmwf.int/publications/newsletters/pdf/88.pdf (last access: 29 May 2015), 2000. 512

Mahfouf, J., Bergaoui, K., Draper, C., Bouyssel, F., Taillefer, F., and Taseva, L.: A comparison of two off-line soil analysis schemes for assimilation of screen level observations, J. Geophys. Res, 114, D08105, doi:10.1029/2008JD011077, 2009. 510, 517

Marthews, T. R., Quesada, C. A., Galbraith, D. R., Malhi, Y., Mullins, C. E., Hodnett, M. G., and Dharssi, I.: High-resolution hydraulic parameter maps for surface soils in tropical South America, Geosci. Model Dev., 7, 711–723, doi:10.5194/gmd-7-711-2014, 2014. 515

SOILD
2, 505–535, 2015

Mercado, L., Huntingford, C., Gash, J., Cox, P., and Jogireddy, V.: Improving the representation of radiation interception and photosynthesis for climate model applications, Tellus B, 59, 553–565, 2007. 511

Naeimi, V., Scipal, K., Bartalis, Z., Hasenauer, S., and Wagner, W.: An improved soil moisture retrieval algorithm for ERS and METOP scatterometer observations, IEEE Trans. Geosci. Rem. Sens., 47, 1999–2013, doi:10.1109/TGRS.2008.2011617, 2009. 514

Peters-Lidard, C., Blackburn, E., Liang, X., and Wood, E.: The effect of soil thermal conductivity parameterization on surface energy fluxes and temperatures, J. Atmos. Sci., 55, 1209–1224, 1998. 513

Reichle, R. H., Kumar, S. V., Mahanama, S. P., Koster, R. D., and Liu, Q.: Assimilation of satellite-derived skin temperature observations into land surface models, J. Hydrometeorol., 11, 1103–1122, 2010. 516

Rudiger, C., Albergel, C., Mahfouf, J.-F., Calvet, J.-C., and Walker, J. P.: Evaluation of the observation operator Jacobian for leaf area index data assimilation with an extended Kalman filter, J. Geophys. Res.-Atmos., 115, D9, doi:10.1029/2009JD012912, 2010. 508

Schaap, M. G. and Leij, F. J.: Database-Related Accuracy and Uncertainty of Pedotransfer Functions, Soil Science, pp. 765–779, 1998. 515

Schneider, S., Wang, Y., Wagner, W., and Mahfouf, J.-F.: Impact of ASCAT soil moisture assimilation on regional precipitation forecasts: A case study for Austria, Mon. Weather Rev., 142, 1525–1541, 2014. 507

Timbal, B., Power, S., Colman, R., Viviand, J., and Lirola, S.: Does soil moisture influence climate variability and predictability over Australia?, J. Climate, 15, 1230–1238, 2002. 507

van Genuchten, M.: A closed-form equation for predicting the hydraulic conductivity of unsaturated soils, Soil Sci. Soc. Am. J, 44, 892–898, 1980. 510, 514

Walker, J. and Rowntree, P. R.: The effect of soil moisture on circulation and rainfall in a tropical model, Q. J. Roy. Meteorol. Soc., 103, 29–46, doi:10.1002/qj.49710343503, 1977. 507

Weisheimer, A., Doblas-Reyes, F., Jung, T., and Palmer, T.: On the predictability of the extreme summer 2003 over Europe, Geophys. Res. Lett., 38, L05704, doi:10.1029/2010GL046455, 2011. 507

SOILD

2, 505–535, 2015

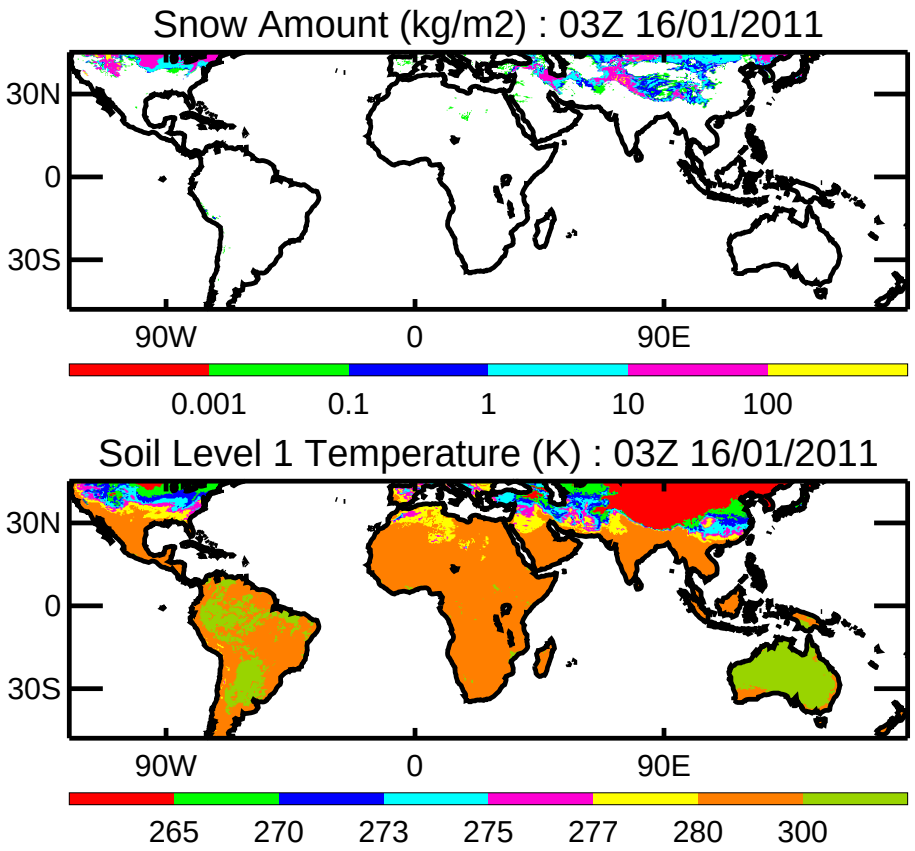

Figure 1. Initial conditions for model snow amount (top panel) and level 1 soil temperature (lower panel) at 3Z 16 January 2011.

SOILD
2, 505–535, 2015

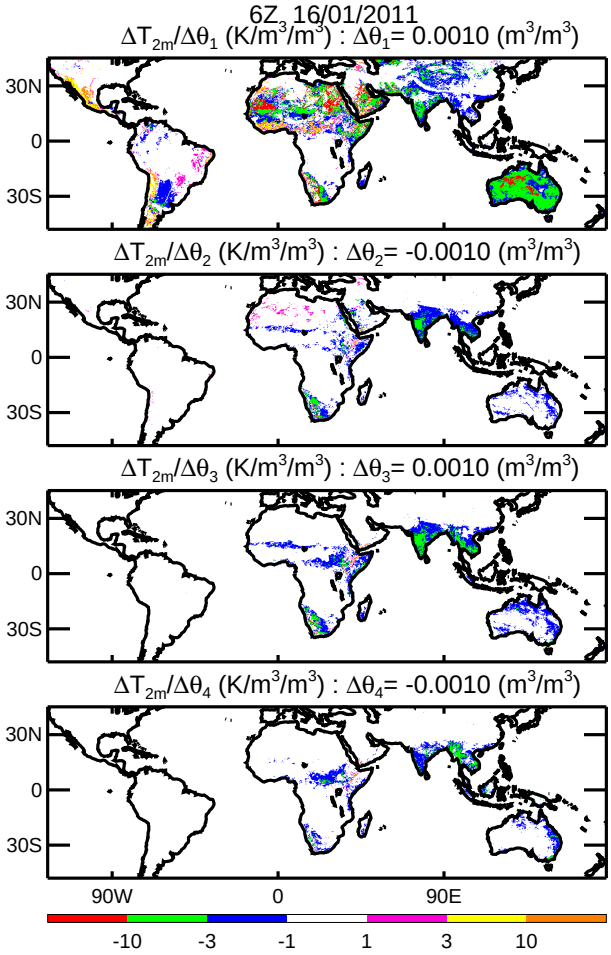

SOILD
2, 505–535, 2015

Analysis of the observation operator in a soil moisture analysis scheme

I. Dharssi et al.

Figure 2. Example of the computed Jacobians of screen level temperature with respect to volumetric soil moisture in the four model soil layers. The Jacobians are valid at 6Z 16 January 2011 and are calculated using three hour long perturbed forecasts with initial soil moisture perturbations of magnitude $|\Delta\theta_l| = 10^{-3}\,\mathrm{m}^3\,\mathrm{m}^{-3}$. The sign of $\Delta\theta_l$ can be positive or negative and for illustration is alternated between soil layers.

SOILD
2, 505–535, 2015

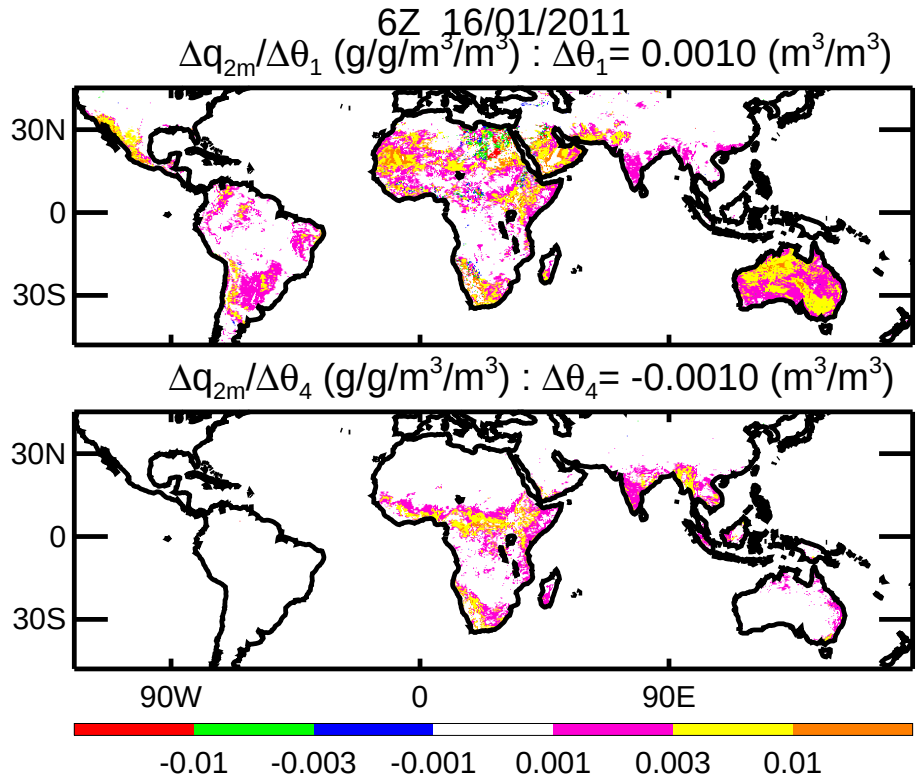

Figure 3. The computed Jacobians of screen level specific humidity with respect to volumetric soil moisture in soil layers 1 and 4. The Jacobians are valid at 6Z 16 January 2011 and are calculated using three hour long perturbed forecasts with soil moisture perturbations of magnitude $10^{-3}\,m^3\,m^{-3}$.

SOILD
2, 505–535, 2015

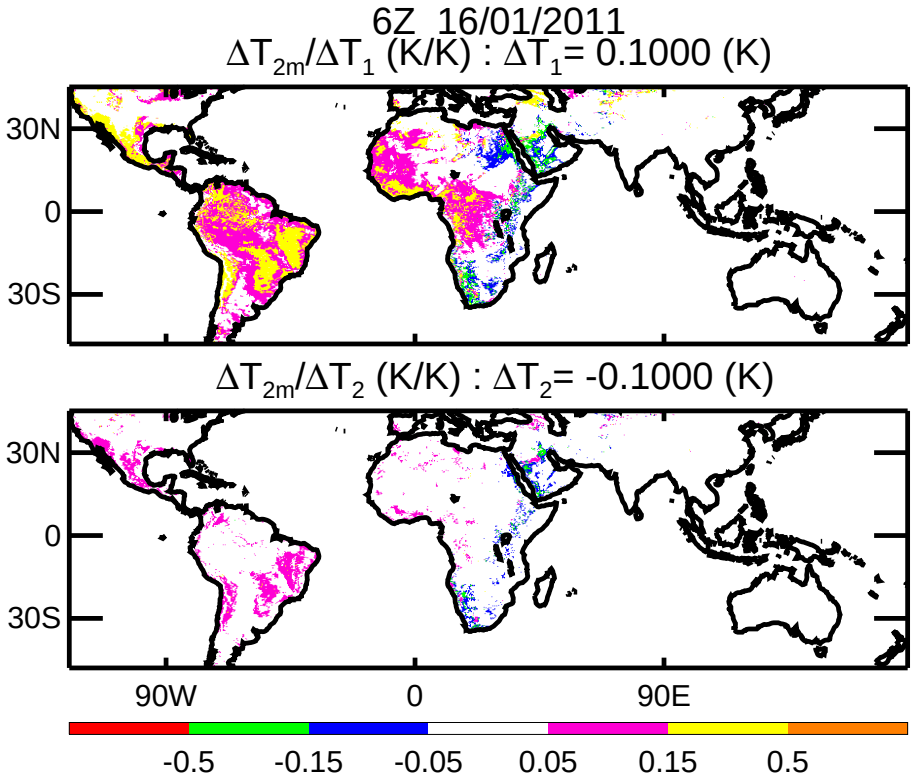

Figure 4. The computed Jacobians of screen level temperature with respect to soil temperature in the top two model soil layers. The Jacobians are valid at 6Z 16 January 2011 and are calculated using three hour long perturbed forecasts with soil temperature perturbations of magnitude 0.1 K.

SOILD
2, 505–535, 2015

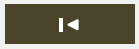

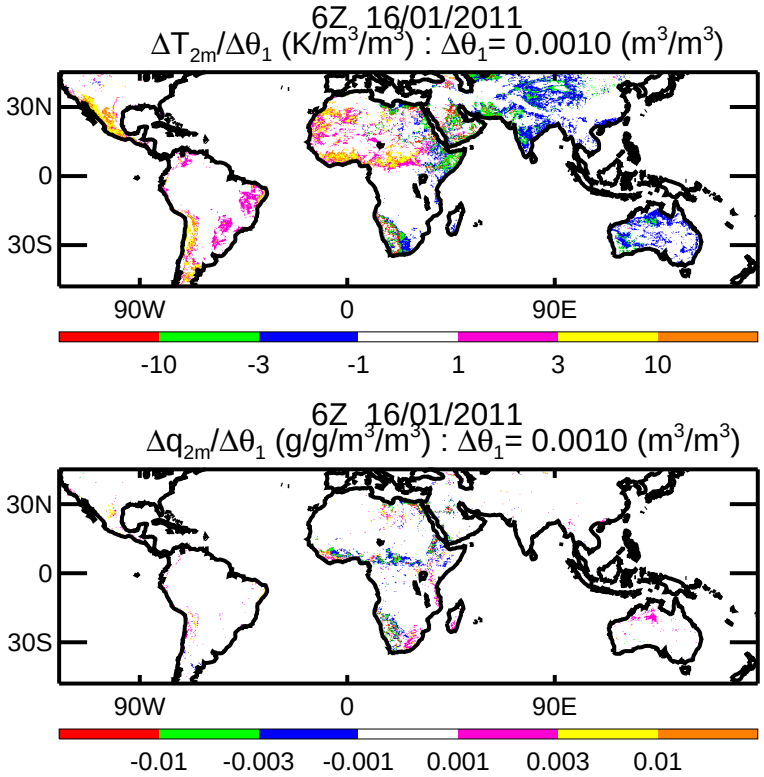

Figure 5. The computed Jacobians when bare soil evaporation is switched off for screen level temperature (top panel) and specific humidity (lower panel) with respect to volumetric soil moisture in the model surface soil layer. This figure can be compared with the top panels of Figs. 2 and 3.

SOILD
2, 505–535, 2015

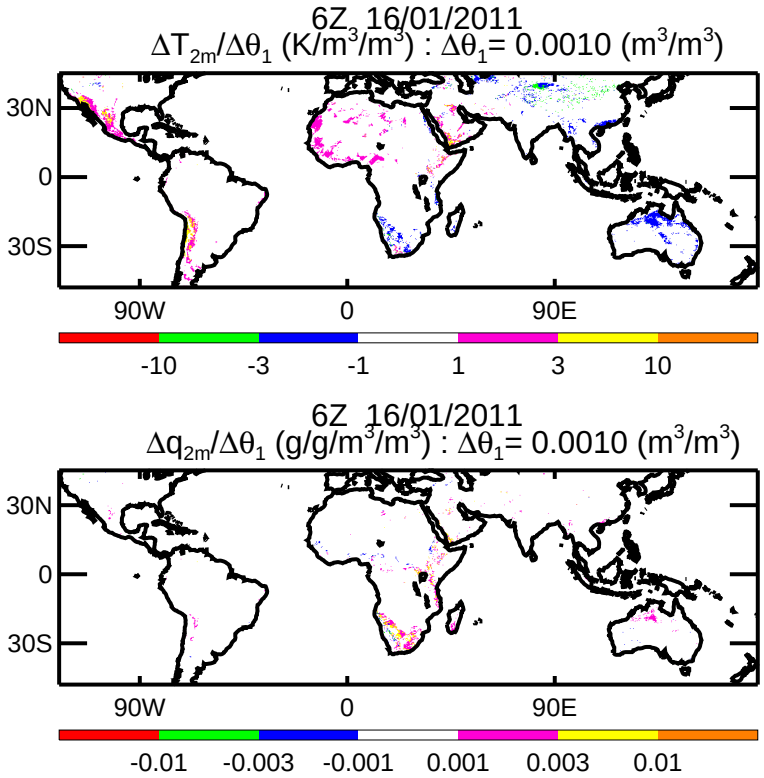

Figure 6. The computed Jacobians of screen level temperature (top panel) and specific humidity (lower panel) with respect to volumetric soil moisture in the topmost model soil layer when bare soil evaporation is switched off and the parameterisation of soil thermal conductivity is modified so that it it independent of soil moisture. The Jacobians are valid at 6Z 16 January 2011 and are calculated using three hour long perturbed forecasts with soil moisture perturbations of magnitude $10^{-3}\,m^3\,m^{-3}$. This figure can be compared with Fig. 5 and the top panels of Figs. 2 and 3.

SOILD
2, 505–535, 2015

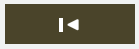

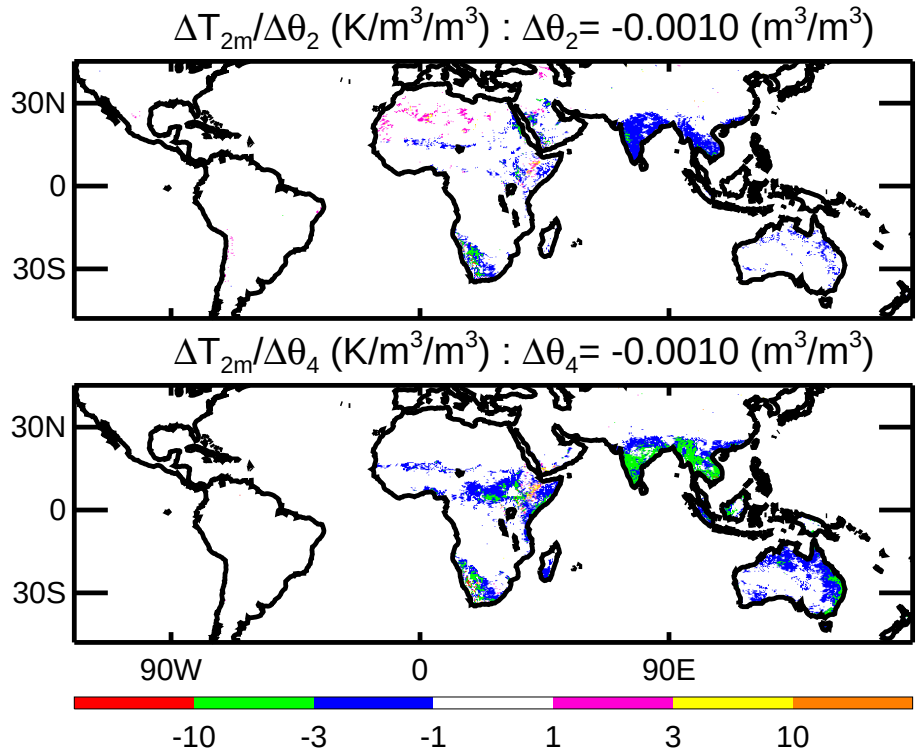

Figure 7. The computed Jacobians of screen level temperature with respect to volumetric soil moisture in soil layers 2 and 4 when the vegetation root depths are doubled. The Jacobians are valid at 6Z 16 January 2011 and are calculated using three hour long perturbed forecasts with soil moisture perturbations of magnitude $10^{-3}\,m^3\,m^{-3}$. This figure can be compared with Fig. 2 which shows the computed Jacobians for the default vegetation root depths.

SOILD
2, 505–535, 2015

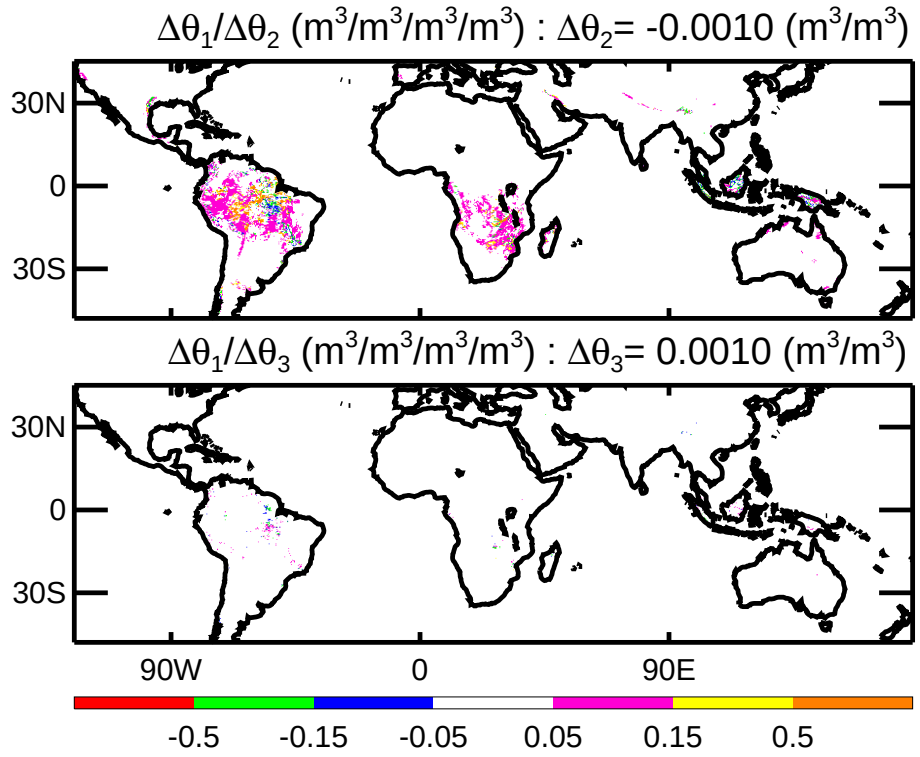

Figure 8. The computed Jacobians of surface volumetric soil moisture with respect to volumetric soil moisture in soil layers 2 and 3. The Jacobians are valid at 6Z 16 January 2011 and are calculated using three hour long perturbed forecasts with soil moisture perturbations of magnitude $10^{-3}\,m^3\,m^{-3}$.

SOILD
2, 505–535, 2015

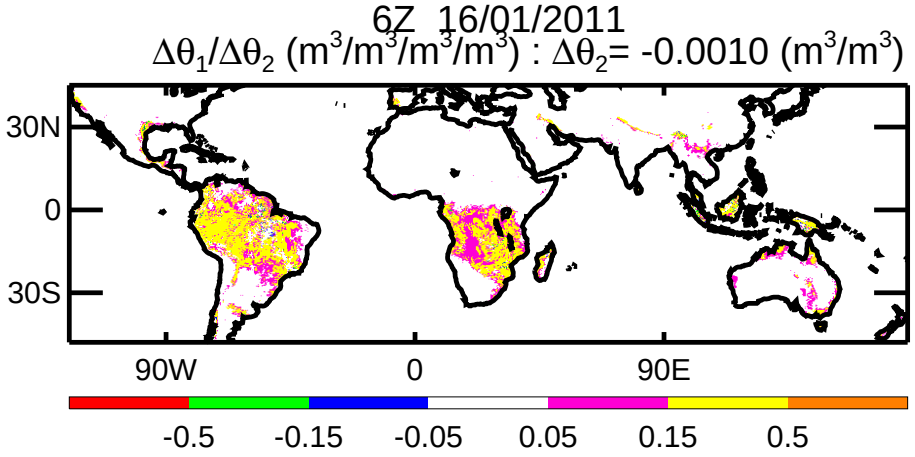

Figure 9. The computed Jacobians of surface volumetric soil moisture with respect to volumetric soil moisture in the second model soil layer when the soil hydraulic conductivity is increases by a factor of ten. The Jacobians are valid at 6Z 16 January 2011 and are calculated using three hour long perturbed forecasts with soil moisture perturbations of magnitude $10^{-3}\,m^3\,m^{-3}$. This figure can be compared with the second panel of Fig. 8.

SOILD
2, 505–535, 2015

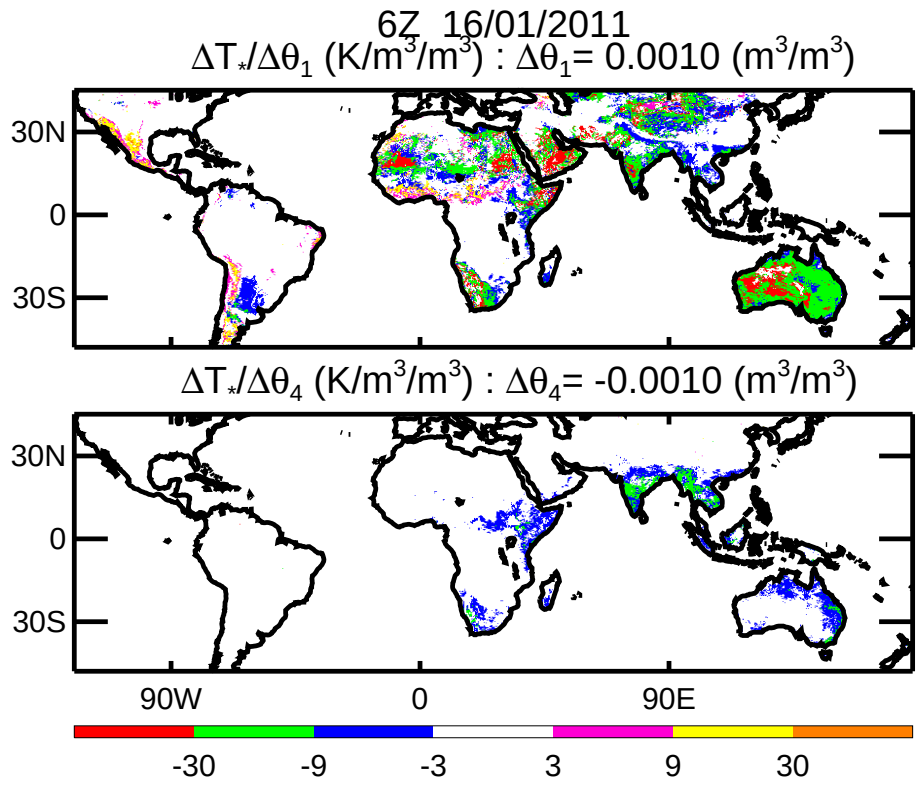

Figure 10. The computed Jacobians of surface skin temperature with respect to volumetric soil moisture in soil layers 1 and 4. The Jacobians are valid at 6Z 16 January 2011 and are calculated using three hour long perturbed forecasts with soil moisture perturbations of magnitude $10^{-3}\,m^3\,m^{-3}$. This figure can be compared with Fig. 2 but note the change in scale.

SOILD
2, 505–535, 2015

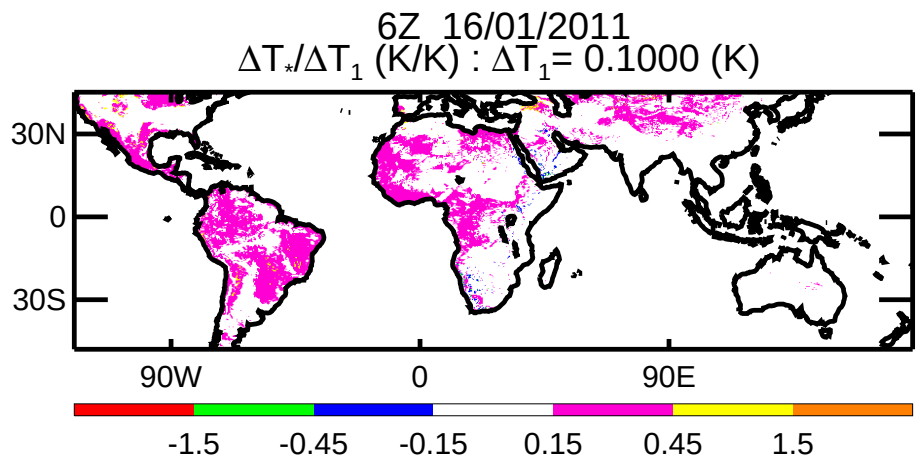

Figure 11. The computed Jacobians of surface skin temperature with respect to soil temperature in soil layer 1. The Jacobians are valid at 6Z 16 January 2011 and are calculated using three hour long perturbed forecasts with soil temperature perturbations of magnitude 10^{-1} K. This figure can be compared with Fig. 4 but note the change in scale.

SOILD
2, 505–535, 2015

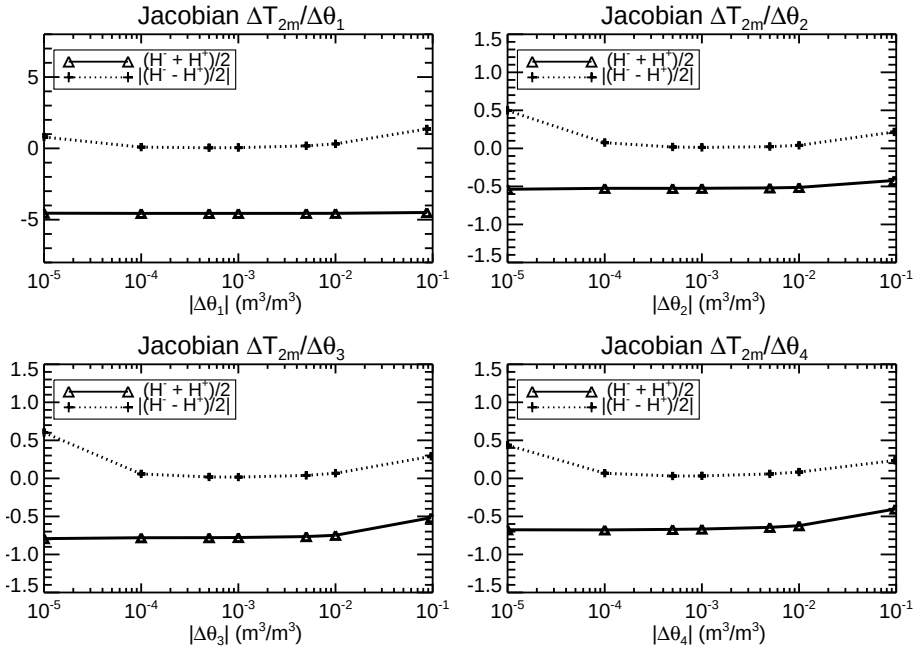

Figure 12. The sensitivity of the calculated Jacobians for screen level temperature to the magnitude of the volumetric soil moisture perturbations $|\Delta\theta_l|$ in soil layer l. H^- represents Jacobian values calculated using a negative perturbation while H^+ represents Jacobian values calculated using a positive perturbation. For a well behaved EKF system $|H^- - H^+|$ should be close to zero. The dotted line shows $|H^- - H^+|/2$ averaged over the Australia region while the solid line shows $(H^- + H^+)/2$ averaged over Australia. The results indicates that the system is well behaved for $|\Delta\theta_l|$ values in the range of 10^{-4} to $10^{-2}\,m^3\,m^{-3}$.

SOILD
2, 505–535, 2015

Analysis of the observation operator in a soil moisture analysis scheme

I. Dharssi et al.